Original Article

Investigating Integrated Multilevel Converter for Switched Reluctance Motor Drives in Hybrid Electric Vehicles

Sajjad Niromand

MSc, Department of Electrical Power Engineering, Khomeini Shahr Branch, Islamic Azad University, Khomeini Shahr, Iran.

Abstract

The present study offers a multilevel converter for switched reluctance motors (SRMs) comprised of an asymmetrical half-bridge converter and a front-end circuit and it is applied for the plug-in hybrid electric vehicles (PHEV). Several operation states can be obtained by changing the on-off statuses of the front-end circuit's switches. In the generator's drive state, the battery's bank is applied for elevating the phase voltage in line with quick evocation and demagnetization. In the battery drive state, the converter is configured as a four-level converter and the capacitor is used as an extra charge capacitor for producing the multilevel output voltage that causes an increase in the torque capability. The operational states suggested for the drive are explained and the phase flow and voltage are each analyzed in details. The battery charge can be naturally obtained by the demagnetization current in motor state and with the regenerative flow in brake state. Moreover, the battery can be charged by an external AC source and/or generator through the proposed converter when the vehicle is in a motionless condition. SRM-based PHEV can work in various speeds through the electrical current's coordination between the generator and battery. In the end, the effectiveness of the proposed converter's topology was simulated on a four-phase 8/6 SRM in PSIM Software so that the capability of the proposed plan can be investigated.

Keywords: quick evocation and demagnetization, front-end circuit, multilevel voltage, flexible battery charge, plug-in hybrid electric vehicle, switched reluctance motor

Introduction

During the past three decades, the switched reluctance motor has gained a particular popularity in the academic and industrial circles. However, the switched reluctance motor is not a new invention and it has a well-known background of about 150 years. In 1969, Nassar suggested the switched reluctance motor for variable-speed launching applications and drew the scientific society's re-attention to this invention [1].

Switched reluctance motors can be considered as a sort of stepper motor. Of course, there are important differences in the structure and control method these motors that has caused the SRMs to be classified within separate groups. Like other reluctance motors, the switched reluctance motors, as well, usually lack magnet in their rotors and stators. This has caused them to have a simple, cheap and robust structure.

Now, the unique properties of SRMs such as their simple and robust structure, high output and the large deal of the power conversion density have turned them into serious rivals for the AC and DC motors. The market potential of this product that can be utilized in many grounds like electric vehicles, home appliances, aerial industries and so forth has also caused expansion of the attentions to the research and development therein.

For HEV and PHEV applications, the permanent-magnet synchronous motors (PMSMs) are considered as a favorable motor drive technology [2] but their magnets are typically derived of the rare earth materials making its vast application in the mass production market limited. As a result, the surrogate technologies demand solutions without the rare earth materials or lower rare earth materials [3].

Switched reluctance motors (SRMs) are well-known for their simpler and stronger structures and absence of any rotor winding or permanent magnet. They can provide a longer service time in harsh environment and be a more cost-effective motor drive choice in contrast to PMSMs [4].

Address for correspondence: Sajjad Niromand, MSc, Department of Electrical Power Engineering, Khomeini Shahr Branch, Islamic Azad University, Khomeini Shahr, Iran.

How to cite this article: Niromand, S. Investigating Integrated Multilevel Converter for Switched Reluctance Motor Drives in Hybrid Electric Vehicles. Arch Pharma Pract 2020;11(S4):91-101.

Furthermore, considering the greater inherent advantages, including high output, high reliability, very excellent error toleration ability and high start torque in initial acceleration [5, 6], SRMs can be envisioned as a competition candidate for the HEV and PHEV electric drivers [7, 8]. In order to improve the reliability of SRM system, the control methods lacking position sensor [9, 10] and the error toleration plans [11, 12] have been developed for the important security applications. In order to reduce the SRM torque's ripple. In order to reduce the SRM's torque ripple, new plans of the direct torque control have been offered for counteracting this issue [13]. In addition, some of the newly emerging technologies have been presented for improving the motor's productivity [14] and reducing vibration [15] in vehicular applications. However, the topology of the SRM's integrated converter has not been developed with several functions for PHEV applications.

Many uses have been made of the converters of the switched reluctance motor. In [16], an SRM converter only with one switch in every phase is capable of providing a high demagnetization voltage in such a way that it increases the output torque of the motor. However, it has been designed for low-cost applications and it cannot achieve a quick evocation. In order to reduce the current increase and decrease times, a quasi-trilevel converter has been developed for SRM drives in [17]. This converter has needs twice or more as much that of the power switches in comparison to the ordinary converters and it increases the cost and complexity of the motor drive to a large extent.

In [18], a sort of magnet-reinforced switched reluctance motor has been introduced and it has a magnet in the evocation pole (PM in E.P). The charge path is in such a way that the flux produced by the winding and the magnet is in the same line when each of the phases is energized and they both reinforce one another. One of the advantages of this structure is that the flux path is in such a way due to the existence of the common poles between the phases that an inverse flux never passes through the permanent magnets hence there is no risk of the magnets' losing of the magnetic flux in this structure.

In an ordinary SRM, the poles' salience brings about various problems in the performance of this motor amongst which the acoustic noise and increase in the rotor's windage losses can be pointed out. In the structure designed in the reference [19], a sort of cylindrical rotor structure has been offered for reducing the windage losses and noise reduction. Although the theoretical investigations performed on the structure show favorable results in terms of the output increase and acoustic noise reduction, the proposed structure's output has not been improved as evidenced in the results experimented in reference [19] rather it is reduced and the acoustic noise has been found improved to a little extent.

Therefore, it can be stated that an integrated multilevel converter has been developed for PHEV applications using a simpler front end circuit (devices with lower power consumption and simpler control algorithm). The modular structure causes the corresponding system to become more compact and suitable for the intended applications. The corresponding converter has been formed of eight asymmetrical half-bridge arms each of which comprised of an IGBT and a diode. For industrial applications, the modular structure is easier in terms of construction and substitution.

The corresponding converter blends the generator and the battery bank only with two IGBTs and two diodes without capacitor and/or extra inductor. Thus, the corresponding converter is more compact and features a better power density and this attribute can be expanded for the higher power applications and multiphase SRMs following which the drive system's productivity can be improved between 2% and 4%. Simulation and test have been carried out in a four-phase 8/6 SRM and the effectiveness of the use of the corresponding drive was confirmed using a front-end circuit.

Materials and Methods:

Performance Principles of the Switched Reluctance Motor (SRM):

The torque produced in these motors can be calculated simply and through the use of the preliminary electromechanical relations. In a rotating reluctance motor, the relations are expressed as below:

$$\Delta w_e = T_e.\Delta\theta \quad (1)$$
$$\Delta w_m = \Delta w'_f \quad (2)$$

Based on the electromagnetic theory, if saturation occurs in none of the core sections, the energy can be expressed by relation (3) for every position of the rotor.

$$w'_f = \frac{1}{2}L(i,\theta).i^2 \quad (3)$$

L(i,θ): stator's inductance
i:stator's flow

the produced electromagnetic torque is obtained from relation (4).

$$T_e = \frac{\partial w_m}{\partial\theta} = \frac{\partial w'_f}{\partial\theta} = \frac{\partial L(i,\theta)}{\partial\theta}.\frac{i^2}{2} \quad (4)$$

Switched Reluctance Motor's Equivalent Circuit:

According to the relations in the above section and considering the idea that the inductance of a SRM is a function of the rotor's current and position hence nonlinear in practice, the offering of a simple equivalent circuit for this type of the motors is infeasible. In this section and disregarding the mutual interphase inductance, an approximate equivalent circuit has been offered for these motors.

$$V = R_s i + \frac{d\lambda(\theta,i)}{dt} \quad (5)$$
$$\lambda = L(i,\theta).i \quad (6)$$

$$V = R_s i + \frac{d(L(i,\theta)i)}{dt} = R_s i + L(\theta,i)\frac{di}{dt} + i\frac{d\theta}{dt}\frac{dL(i,\theta)}{d\theta} = R_s i + L(\theta,i)\frac{di}{dt} + \frac{dL(i,\theta)}{d\theta}\omega_m i \quad (7)$$

The Studied Converter:

The Corresponding Multilevel Integrated Converter for PHEVs:

As it has been shown in figure (1), the proposed power converter was constructed with a front-end circuit and an ordinary asymmetrical half-bridge converter.

The front-end circuit includes an AC electric machine (G/M), an IGBT one-bridge inverter/rectifier, a capacitor (C) and a battery bank (B). In addition, a relay (J), two IGBTs (S_{01} and S_{02}) and two diodes (D_{01} and D_{02}) have been used in the combination for the achievement of the various operational states. IGBTs have been used in the converter with a fast recovery antiparallel diode. In the drive of the corresponding drive, the battery bank (B) is applied for the generator's power source link for achieving multilevel voltage for generator drive's operation and the capacitor (C), as well, is used for heightening the DC link's voltage for battery's drive operation. The demagnetization current and the brake current can directly provide the battery charge with the feed returning to the feed source with the existence of several antiparallel diodes in S01 switch. They can be flexibly obtained through controlling the on-off statuses of the switch tools (S01 and S02) in the front-end circuit.

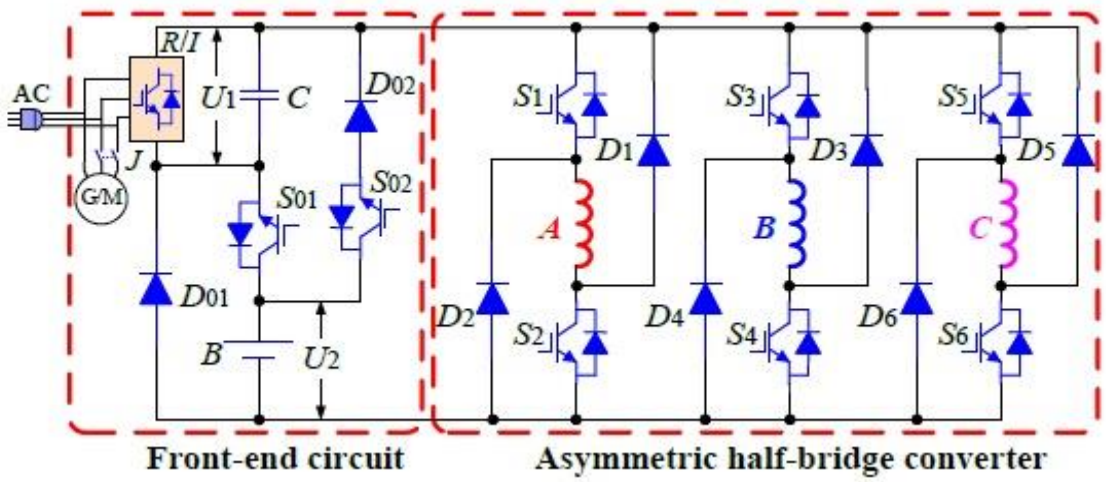

Figure (1): the integrated converter fed with the front-end circuit [20]

The Intended Converter's Operational Modes:

Figure (2) illustrates the four operational states of the corresponding converter and they can be flexibly obtained through controlling the on-off statuses of the switch tools (S01 and S02) in the front-end circuit.

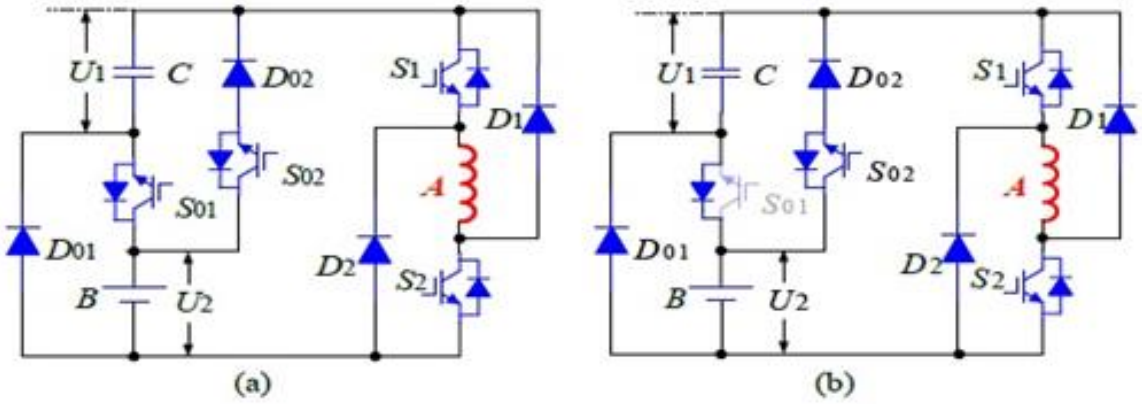

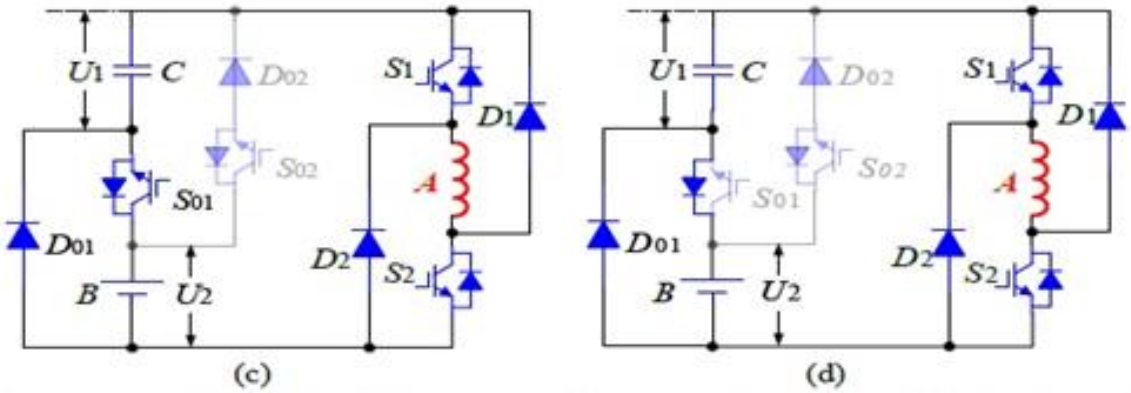

Figure (2): operational modes of the two front sources' circuit (a) state 1: S01 on and S02 off (a) state 2: S01 off and S02 on (a) state 3: S01 on and S02 on (a) state 4: S01 off and S02 off [20]

Analyzing Phase Voltage and Current:

In a period of flow, every phase is faced with three primary states: 1) evocation state, 2) idle state and 3) demagnetization state. The operational states of the corresponding converter fed with the front-end circuit are different from the ordinary converter in the phase commutation region. Figure (3) displays the relationship between the phase current and phase voltage under various states of the drive source. As it has been shown in figure 3(a), the phase voltage's switch between +U1 and -U1 is without front-end circuit in the ordinary converter whereas the multilevel voltage obtained in the corresponding converter and the quick evocation and fast demagnetization are obtained both in the generator's drive states as demonstrated in figures 3(b) and 3(c).

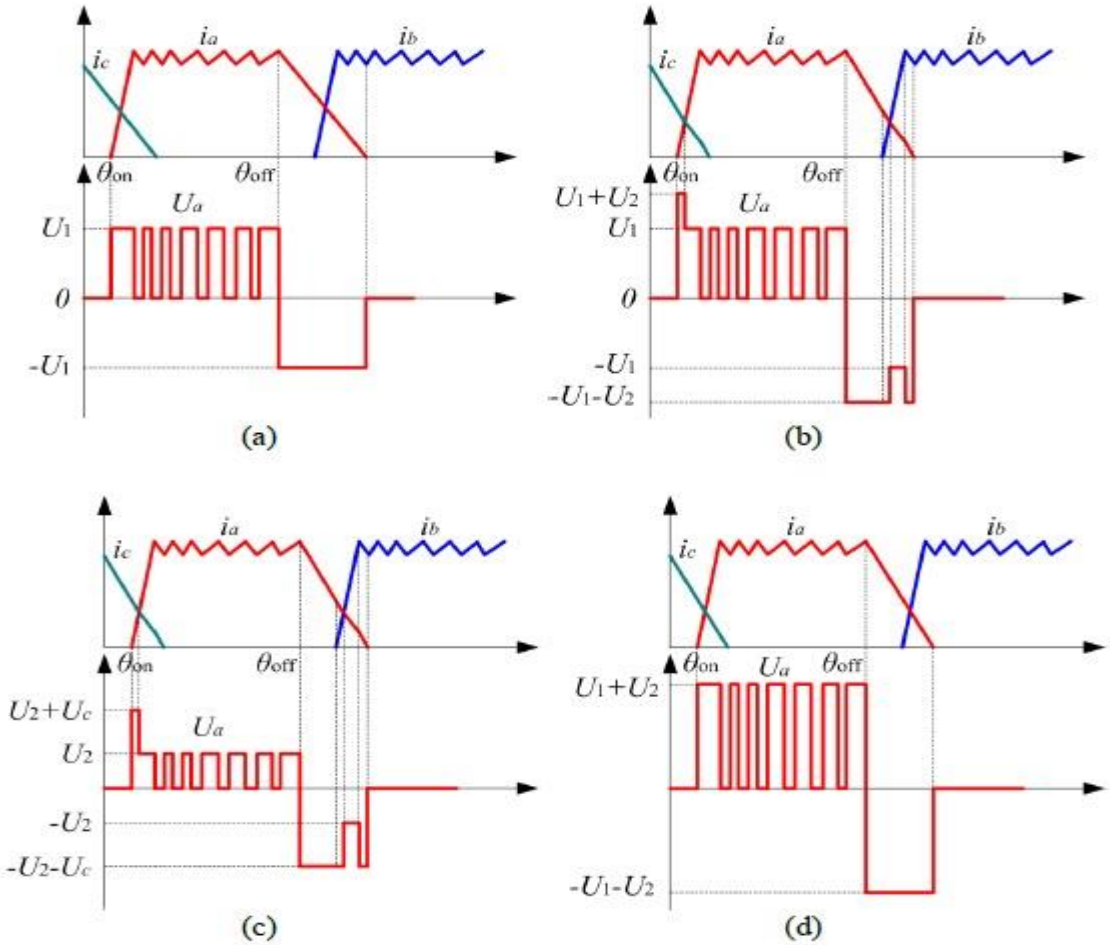

Figure (3): phase voltage and phase current (a); ordinary converter (b); the drive or generator in the new converter (c) the drive or battery in the new converter (d) drive or the two sources in the new converter [20]

The Energy Exchanges between the Two Sources:

When PHEV is under stop conditions, the capacitor C can change the battery bank B by controlling the power switches in the drive circuit. Two work stages should be existent under these conditions; in the first work stage, switches S1~S6 are turned on in a single moment for providing all the on phase windings with energy. In the second work stage, the S1~S6 are turned off at a single time and the energy stored in the phase windings in capacitor C and battery bank B are discharged through D1~D6 diodes. In this process, the battery bank can be flexibly charged by the capacitor's energy. The phase current of the first work stage can be expressed as below:

$$i_{k1}(t) = I_{k0} + \frac{I_{km} - I_{k0}}{DT} t \quad (8)$$

Where, i_{k0}, i_{km}, T and D are respectively the initial phase current, maximum phase current, period and cycle of switching.

$$i_{k2}(t) = I_{km} - \frac{I_{km} - I_{k0}}{(1-D)T}(t - DT) \quad (9)$$

Using three phase windings, the maximum and the minimum DC link current becomes equal to:

$$\begin{cases} I_{\max} = I_{am} + I_{bm} + I_{cm} \\ I_{\min} = I_{a0} + I_{b0} + I_{c0} \end{cases} \quad (10)$$

Therefore, the battery charging flow in the second stage can be expressed in the following form:

$$i_s(t) = I_{\max} - \frac{I_{\max} - I_{\min}}{(1-D)T}(t - DT) \quad (11)$$

SRM Drive's Control Method:

The hard control of the current and the pulse control of the voltage are applied as two essential plans in the SRM drive's control model. Considering the given speed of ω^*, the hard control of the current is conducted in the low speed and the voltage pulse control is carried out in a higher speed. The motor speed can be measured using a speed calculator by means of an encoder. The speed error is processed through a PI controller for regulating the motor's speed. The on-off angle is determined by the position detector for phase commutation control. In the hard current control plan, the phase current is navigated by a current controller. The current of the source i^* has been derived of a speed controller. The momentary phase current is measured using the current sensors and fed into the logical threshold for the calculation of i_{max} and i_{min} determining the switch status in every region of the phase turn-on. In voltage pulse control plan, the turn-on angle has been derived of the angle controller and the regulation is conducted according to the momentary speed.

RESULTS:

Simulation Diagram's Block:

In order to investigate the topology capability of the corresponding converter, use has been made of a low-power four-phase 8/6 SRM. The motor's parameters have been presented in table (1). Simulation model of the motor system in PSIM software is as shown in figure (4). It has to be noted that the upper section of the model in this figure is reflective of a circuit consisted of AC network, AC-DC converter and the capacitor connected to the DC section of AC-DC converter.

Table 1: parameters of the four-phase 8/6 motor [20]

Parameters	Value
Phase number	3
Stator/rotor poles	12/8
Rated power (W)	750
Rated speed (r/min)	1500
Phase resistor (Ω)	3.01
Minimum phase inductance (mH)	27.2
Maximum phase inductance (mH)	256.7
Rotor outer diameter (nmi)	55
Rotor inner diameter (mm)	30
Stator outer diameter (mm)	102.5
Stator inner diameter (mm)	55.5
Stack length (mm)	80
Stator arc angle (deg)	14
Rotor arc angle(deg)	16

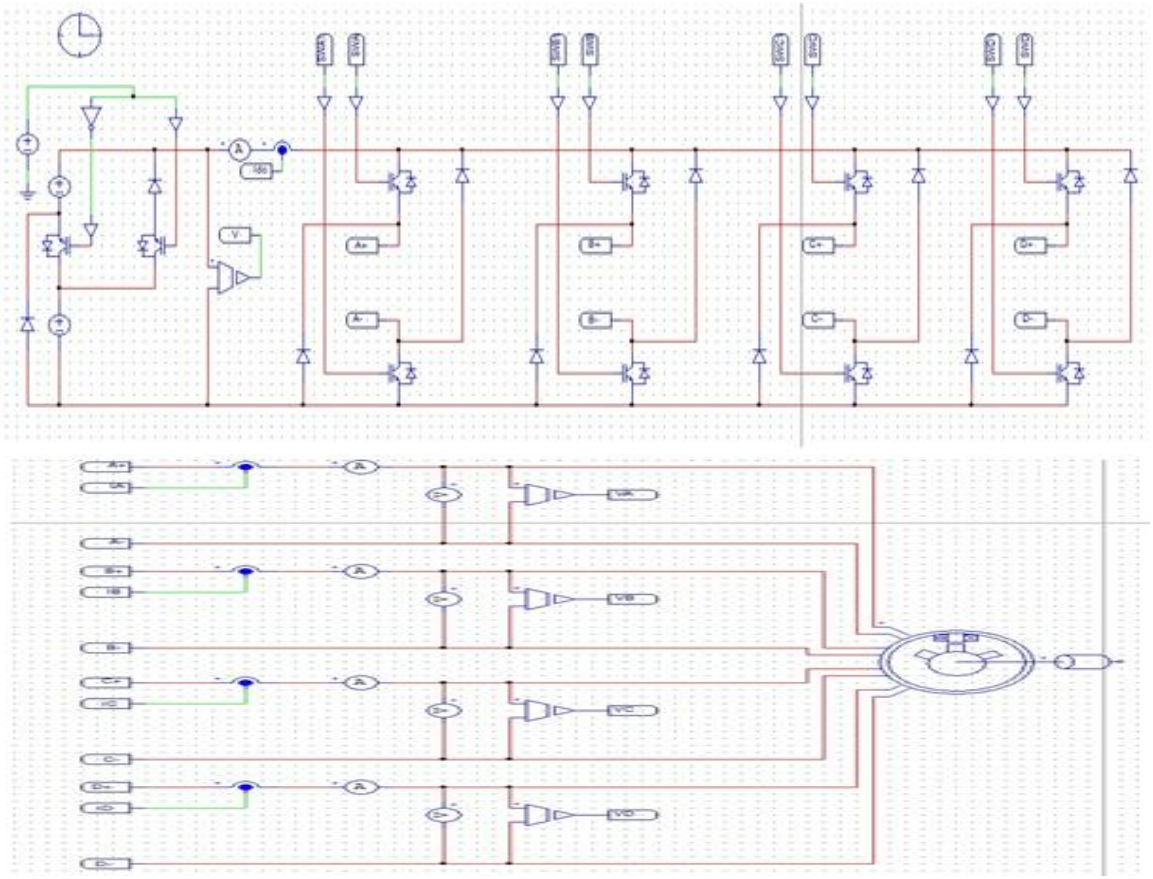

Figure (4): parameters of the four-phase 8/6 motor [20]

Simulation in Low Speed:

In simulation, the generator's voltage and the battery's voltage have been respectively set at 80V and 48V. the hysteresis width of the current has been set at 0.1A. The load is 1.8 newton meters. Figure (5) exhibits the phase current, phase voltage and battery current at 300rpm. The phase voltage and the phase current have been shown for a common converter without front-end circuit in figure 5(a). Based on this figure, the phase voltage A varies between 80 and -80 as a result of the switching states. Additionally, based on the reference speed of 300rpm, the amount of every phase's current is equal to 2 amperes with a ripple in a range of 0.1 as a result of the hysteresis control ring. The results of the generator's drive state has been shown in figure 5(b). In this situation, the S01 and S02 keys are both off. As it is seen in figure 5(b), the battery bank causes an increase in phase voltage from 80V to 128V in the commutation region for obtaining quick evocation and fast demagnetization. Moreover, the battery is also charged in this state by the demagnetization current. Figure 5(c) demonstrates the results of the simulation in the battery drive state. In this state, the S01 key is off and the S02 key is on and the converter has been again configured in the form of a four-level converter. In this state, the upper battery of the circuit is utilized in the evocation region as an additional charge supply for increasing the phase voltage and creating fast current and, in the demagnetization region, for rapid reduction of the current. Furthermore, in this section, the battery bank is discharged in the evocation region and charged in the demagnetization region. In the end, figure (3-5d) exhibit the simulation results in the drive state of the two sources which includes turned-on S01 and turned-off S02. The results of this section, as well, are like those of the figure 5(a) with the difference being that the phase voltage is equal to 128V in this section.

As it is observed in figure (5) based on the results of the various study cases, every phase's current is charged from zero and increased up to 2 amperes; in figure 5(a), the phase current's reaching of two amperes is more likely in contrast to the results of the other cases because, in the case investigated in figure 5(a), the voltage is equal to 80V in this instant while it is equal to 128V in other cases in the beginning of every phase's connection to DC and this has caused the lower amount of time needed for the phase current's reaching of two amperes in this case as compared to the others in figure 5(a).

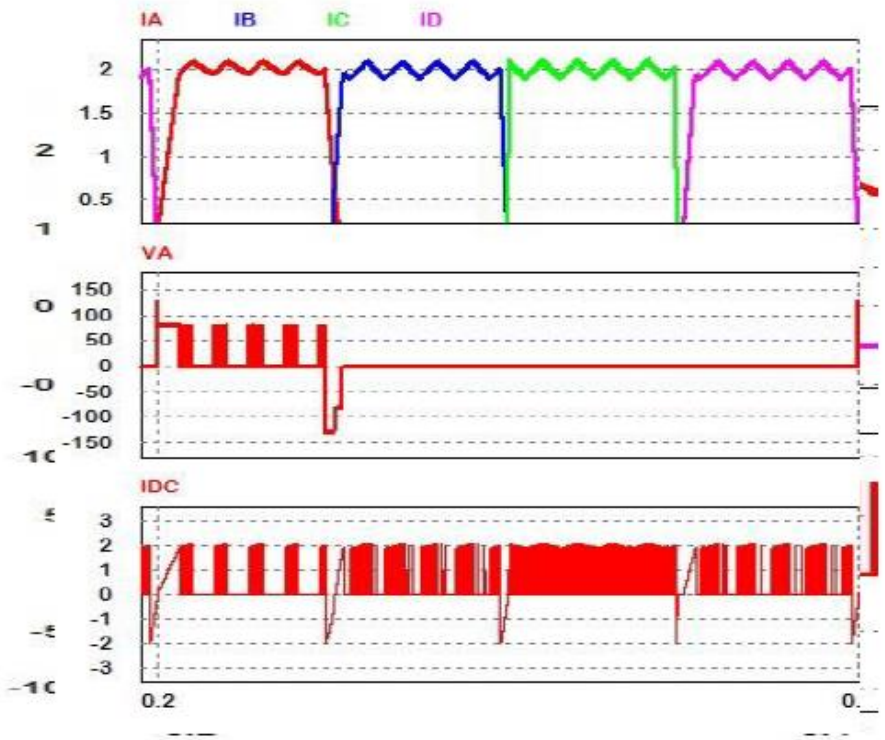

(a)

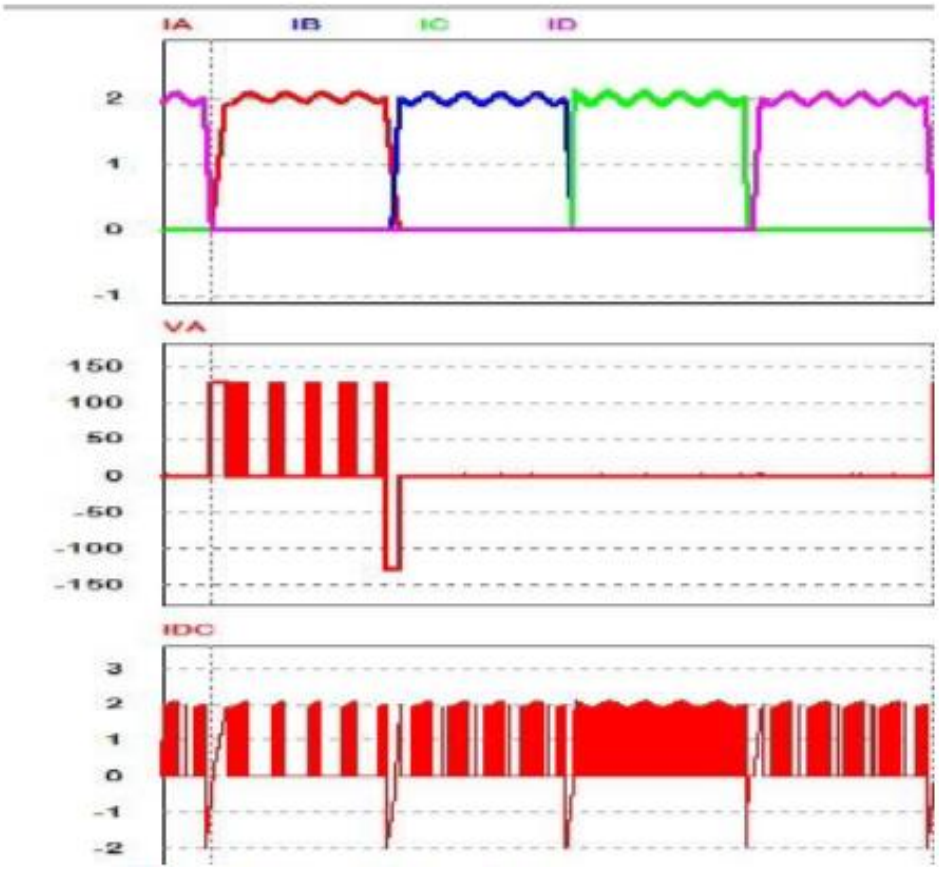

(b) & (c)

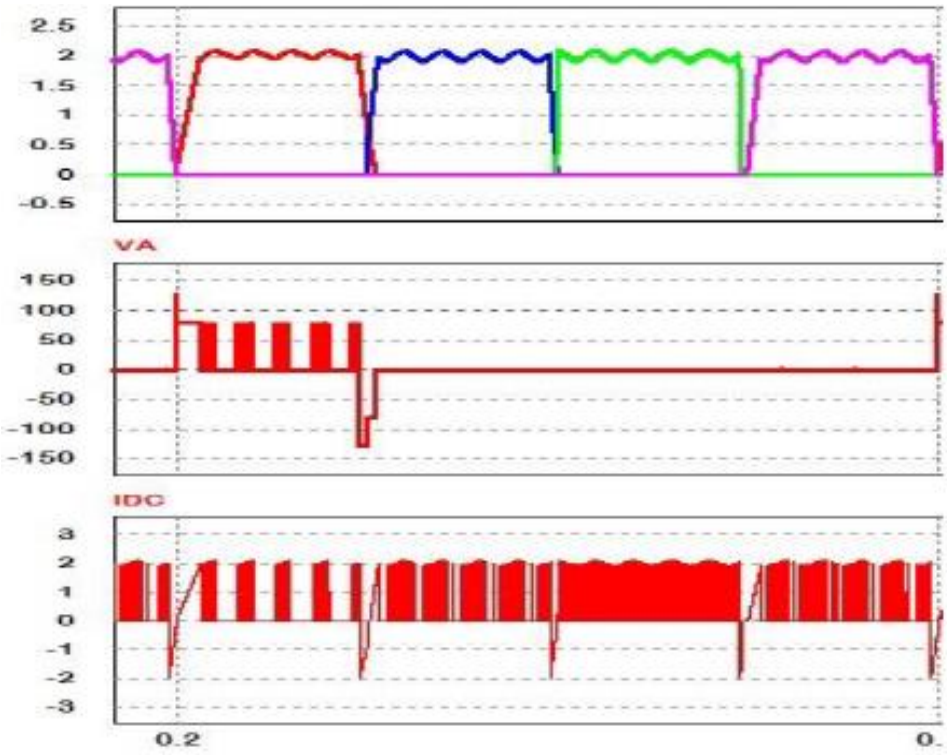

(d)

Figure (5): the results of the simulation for low-speed operation; a) the results obtained from the common converter; b) the generator's drive state; c) the battery's drive state and d) the battery and generator's drive state

High-Speed Simulation:

Figure (6) illustrates the simulation results in 1500rpm. The fast evocation and rapid demagnetization have been obtained along with battery charge in the generator's drive state in high-speed operation and this has been shown in figure 6(a). in figure 6(b), the generator and the battery bank are connected in series to the motor's drive and the battery bank is alternatively charged and discharged.

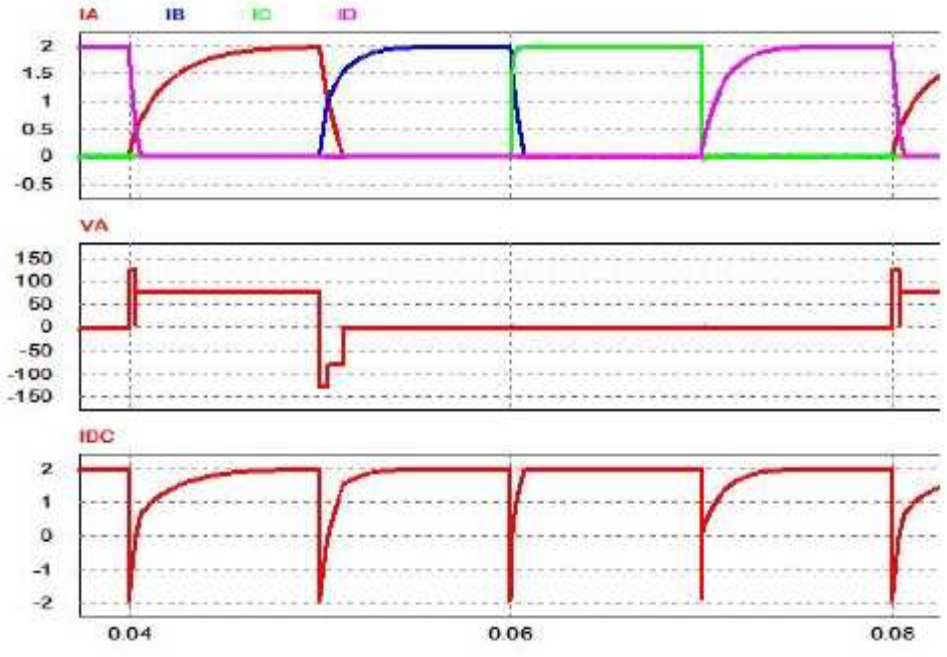

(a)

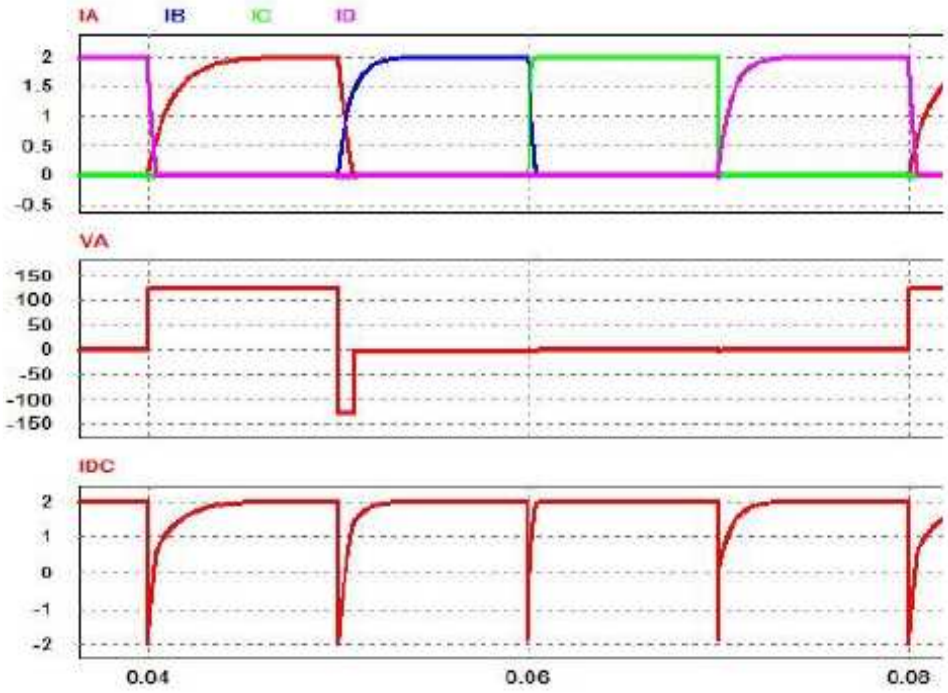

(b)

Figure (6): the results of the simulation for high-speed operation; (a) generator's drive state and (b) battery and generator's drive

The Results of Simulating Battery Charging by an External AC Source under Stop Conditions:

When the motor is in stop conditions, the battery charge can be flexibly obtained by the external AC source and/or generator. Figure (7) displays the simulation results for the battery charge in brake state wherein the switching frequency has been set at 500 hertz for 0.5 and 0.6 work cycles. When all the switches are on at a single time, the four windings of the phases take energy from the very external source and/or generator and the phase current is increased as long as the switches are off. Afterwards, the energy stored in the motor's winding is transferred to the battery bank. In this process, the battery bank can be charged flexibly using the switching frequency control and work cycle.

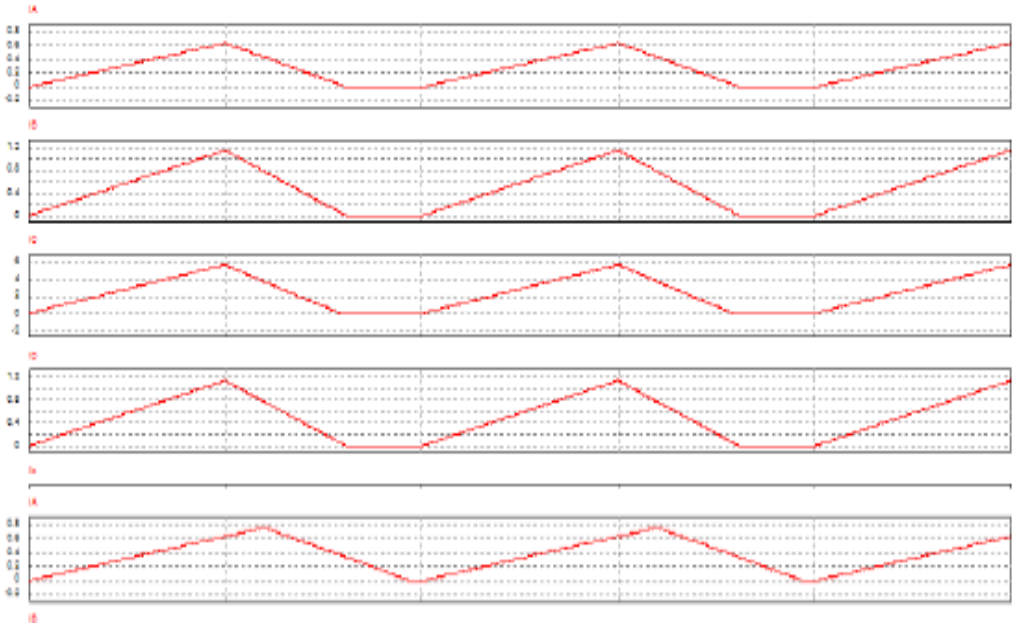

(a)

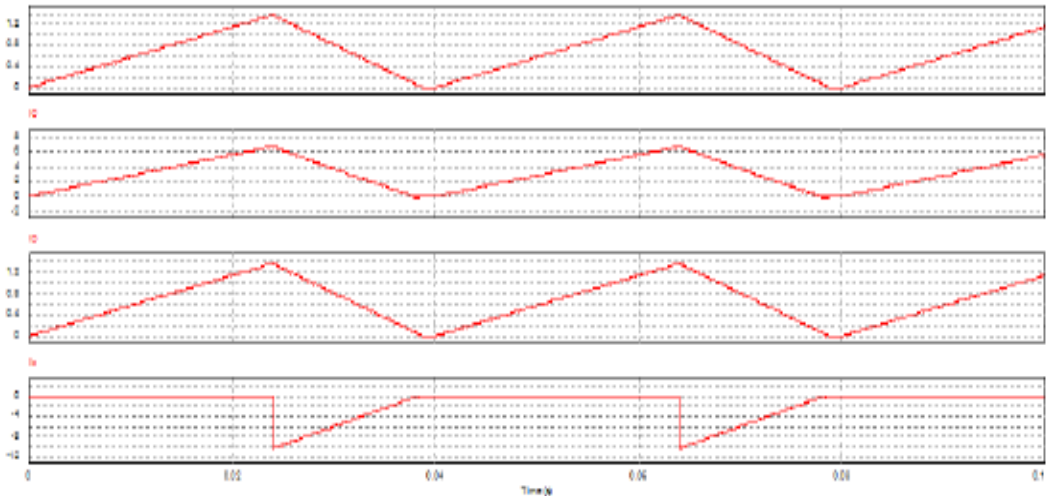

(b)

Figure (7): the results of the simulation for battery charge under stop conditions; (a) work cycle set at 0.5 and (b) work cycle set at 0.6

Comparison with the Common Asymmetrical Converter

As shown in the simulation results, the corresponding converter causes an increase in the phase voltage in the commutation region in comparison to the ordinary asymmetrical converter for obtaining the quick evocation and fast demagnetization.

Table 2: the comparison of the ordinary converter and the corresponding converter

Converter type	Phase voltage	Evocation and demagnetization
Ordinary	80	Slow
Corresponding converter	128	Fast

Conclusion:

In this study, an SRM drive fed by a modular front-end circuit was presented herein for PHEV application. The multilevel and multistate voltage can be obtained by controlling the switches' on-off statuses in the front-end circuit. The evocation states and demagnetization modes of the corresponding converter have been offered and the voltage and current have been analyzed in various work modes in details. In comparison to the existing plans, the improved front-end circuit has been applied for performing multilevel and multistate voltage operations using the devices with lower power and the simpler control algorithm. The topology is simpler considering the modular structure for the construction and substitution. The corresponding converter blends the generator and the battery bank in this drive system only with two IGBTs and two diodes without adding capacitor and without extra inductors. Therefore, the corresponding converter is more compact and features a better power density. This can be expanded for the higher power applications and multistage SRMs. The evocation and demagnetization have been accelerated in comparison to the ordinary converters. The torque capability has been improved by 30% due to the multilevel voltage without torque ripple increase. The motor system's productivity has been improved between 2% and 4%. In addition, the battery can be charged flexibly under stop, brake and drive conditions without any need for the external charging instruments. The corresponding SRM drive has shown a good scalability for the manufacturing of the high voltage and high power systems, if needed.

References

1. Abbasian, M., Designing and construction of a two-stator switched reluctance machine with rearrangement of the microforces, PhD thesis, power and computer department, Industrial Univeristy of Isfahan, 2010.
2. Sant AV, Khadkikar V, Xiao W, Zeineldin HH. Four-axis vector-controlled dual-rotor PMSM for plug-in electric vehicles. IEEE Transactions on Industrial Electronics. 2014 Dec 31;62(5):3202-12.
3. Chiba A, Kiyota K, Hoshi N, Takemoto M, Ogasawara S. Development of a rare-earth-free SR motor with high torque density for hybrid vehicles. IEEE Transactions on Energy Conversion. 2014 Aug 27;30(1):175-82.
4. Kiyota K, Kakishima T, Chiba A. Comparison of test result and design stage prediction of switched reluctance motor competitive with 60-kW rare-earth PM motor. IEEE Transactions on Industrial Electronics. 2014 Feb 5;61(10):5712-21.
5. Ye J, Bilgin B, Emadi A. An extended-speed low-ripple torque control of switched reluctance motor drives. IEEE Transactions on Power Electronics. 2014 Apr 14;30(3):1457-70.
6. Ye J, Bilgin B, Emadi A. An offline torque sharing function for torque ripple reduction in switched reluctance motor drives. IEEE Transactions on energy conversion. 2015 Jan 9;30(2):726-35.
7. Gan C, Wu J, Yang S, Hu Y. Phase current reconstruction of switched reluctance motors from dc-link current under double high-frequency pulses injection. IEEE Transactions on Industrial Electronics. 2014 Oct 21;62(5):3265-76.
8. Bilgin B, Emadi A, Krishnamurthy M. Comprehensive evaluation of the dynamic performance of a 6/10 SRM for traction application in PHEVs. IEEE Transactions on Industrial Electronics. 2012 Apr 26;60(7):2564-75.
9. Hu KW, Chen YY, Liaw CM. A reversible position sensorless controlled switched-reluctance motor drive with adaptive and intuitive commutation tunings. IEEE Transactions on Power Electronics. 2014 Jul 24;30(7):3781-93.

10. Ofori E, Husain T, Sozer Y, Husain I. A pulse-injection-based sensorless position estimation method for a switched reluctance machine over a wide speed range. IEEE Transactions on Industry Applications. 2015 Apr 6;51(5):3867-76.
11. Hu Y, Gan C, Cao W, Li W, Finney SJ. Central-tapped node linked modular fault-tolerance topology for SRM applications. IEEE Transactions on Power Electronics. 2015 Mar 18;31(2):1541-54.
12. Hu Y, Gan C, Cao W, Zhang J, Li W, Finney SJ. Flexible fault-tolerant topology for switched reluctance motor drives. IEEE Transactions on Power Electronics. 2015 Sep 7;31(6):4654-68.
13. Ye J, Bilgin B, Emadi A. An extended-speed low-ripple torque control of switched reluctance motor drives. IEEE Transactions on Power Electronics. 2014 Apr 14;30(3):1457-70.
14. Chiba A, Takano Y, Takeno M, Imakawa T, Hoshi N, Takemoto M, Ogasawara S. Torque density and efficiency improvements of a switched reluctance motor without rare-earth material for hybrid vehicles. IEEE Transactions on Industry Applications. 2011 Mar 10;47(3):1240-6.
15. Gan C, Wu J, Shen M, Yang S, Hu Y, Cao W. Investigation of skewing effects on the vibration reduction of three-phase switched reluctance motors. IEEE Transactions on Magnetics. 2015 Jun 3;51(9):1-9.
16. Deriszadeh A, Adib E, Farzanehfard H, Nejad SM. Switched reluctance motor drive converter operating in continuous conduction mode with high demagnetisation voltage. IET power electronics. 2015 Mar 31;8(7):1119-27.
17. Tomczewski K, Wrobel K. Quasi-three-level converter for switched reluctance motor drives reducing current rising and falling times. IET power electronics. 2012 Aug 1;5(7):1049-57.
18. Hwang H, Hur J, Lee C. Novel permanent-magnet-assisted switched reluctance motor (I): Concept, design, and analysis. In2013 International Conference on Electrical Machines and Systems (ICEMS) 2013 Oct 26 (pp. 602-608). IEEE.
19. Kiyota K, Kakishima T, Chiba A, Rahman MA. Cylindrical rotor design for acoustic noise and windage loss reduction in switched reluctance motor for HEV applications. IEEE Transactions on Industry Applications. 2015 Aug 11;52(1):154-62.
20. Gan C, Wu J, Hu Y, Yang S, Cao W, Guerrero JM. New integrated multilevel converter for switched reluctance motor drives in plug-in hybrid electric vehicles with flexible energy conversion. IEEE Transactions on Power Electronics. 2016 Jun 22;32(5):3754-66.